Journal of Chromatography, 480 (1989) 111–127
Elsevier Science Publishers B.V., Amsterdam — Printed in The Netherlands

CHROM. 21 812

USE OF PELTIER THERMOELECTRIC DEVICES TO CONTROL COLUMN TEMPERATURE IN HIGH-PERFORMANCE CAPILLARY ELECTROPHORESIS

R. J. NELSON, A. PAULUS[a], A. S. COHEN, A. GUTTMAN and B. L. KARGER*
Barnett Institute, Northeastern University, Boston, MA 02115 (U.S.A.)

SUMMARY

A temperature control system for high-performance capillary electrophoresis is described utilizing Peltier thermoelectric devices. The thermoelectric devices heat or cool an alumina block which has a high thermal conductivity for efficient heat removal from the external capillary column wall. The heat dissipation characteristics of this device are compared to natural convection and fan cooling by observing the stability of current with time and the dependence of current on applied field. A linear relationship of electroosmotic flow velocity with increasing field is found, indicative of a constant temperature at the inside wall of the capillary. Also, the change in peak shape of horse heart myoglobin as a function of increasing temperature is shown to demonstrate the importance of temperature control in obtaining optimum efficiency.

INTRODUCTION

There is, at present, significant interest in high-performance capillary electrophoresis (HPCE)[1–3]. HPCE can be characterized as a rapid and powerful separation method which is fully complementary to high-performance liquid chromatography (HPLC). The method requires the use of high electric fields (100–300 V/cm) for rapid separations at high efficiencies. Although high fields can result in Joule heating, with the use of narrow-bore capillaries, heat generation and heat dissipation become less problematic.

Thermal effects in HPCE have been recognized, especially in terms of their influence on column efficiency. It has been suggested that for large-bore capillaries (> 100 μm) Joule heating can be responsible for an increase in the height equivalent to a theoretical plate (HETP) at high fields due to a temperature difference between the center of the column and the wall[1,4–12]. Therefore, separations in narrow-bore columns have been recommended to reduce the radial temperature effect within the column bore[4,6,12]. It has also been shown that the overall column temperature can rise to over 70°C even with narrow-bore columns without proper cooling[5].

[a] Present address: Analytical Research, Ciba-Geigy, Basel, Switzerland.

0021-9673/89/$03.50

In order to realize more fully the advantages inherent in HPCE separations, further experimental investigation is needed on the removal of Joule heat from the outer column surface. This heat influences column temperature which affects, among other things, the sample stability, buffer viscosity, chemical equilibria, pH and the resulting migration time for a given species. In short, column temperature influences most of the important physical and chemical parameters involved in HPCE. The temperature at which a separation is performed is determined by both the ambient level (or set temperature of the temperature control system) and the temperature generated by the Joule heating from the applied power. Given the influences that temperature has on a separation, it is important that the column temperature be maintained accurately and precisely for good reproducibility within and between laboratories.

Although thermal effects can be reduced by the use of narrow-bore columns with low conductivity or low concentration buffers, such approaches can have other consequences. For example, buffers of low concentration limit sample loading and a decreased column radius increases the column surface area-to-volume ratio, which can enhance the potential for adsorption effects[1]. In addition, the concentration sensitivity and signal-to-noise for optical detectors will suffer with decreasing column diameter. Many workers would prefer to use columns in the 50 to 100 μm diameter range for improved detectability, ease of handling and column loading[6]. Furthermore, there is a trend toward higher conductivity solutions (*e.g.* micelles, metals, salts) for optimum resolution[5,13–15]. These highly conductive additives can have a profound effect on the current, and thus upon the applied power and heat generated by a particular set of separation conditions.

In this work we describe a solid-state temperature control system that utilizes Peltier thermoelectric modules. These thermoelectric devices have been previously used in conventional slab gel electrophoresis to control temperature[16,17]. In the present system the devices were employed to maintain the temperature of an alumina column support which had a high thermal conductivity and low electrical conductivity. Various column diameters up to 200 μm, and column lengths up to 1 m were examined. The ability of this system to remove heat generated on the column was characterized by studying the dependence of current on applied voltage[5]. The rate of heat removal for the temperature control system was also compared to natural and forced air convection. On the basis of these results, it can be concluded that a temperature control system such as a Peltier device is important to sustain operation at high applied powers and to maintain in a reproducible manner the column temperature at that which is optimum for a given separation.

EXPERIMENTAL

The basic instrumental configuration is shown in Fig. 1. A 60 kV, 500 μA power supply, Model No. PS/MK60P00.5X66 (Glassman High Voltage, Whitehouse Station, NJ, U.S.A.) was used for all experiments. Panel meters were installed which provide digital resolution of 10 V and 0.1 μA. A Model 783A programmable absorbance detector (Applied Biosystems, Foster City, CA, U.S.A.) was used for all temperature studies. The detector was modified to accept fiber optics that were then connected to the machined alumina block (Ceramics Grinding Co., Waltham, MA,

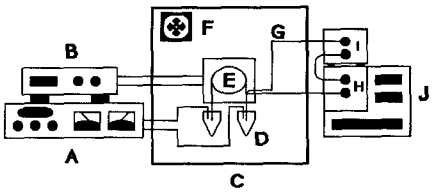

Fig. 1. Diagram of the HPCE instrument: A = Power supply; B = thermoelectric temperature controller; C = black plexiglass light-tight box; D = Eppendorf micro test tubes; E = thermoelectric cooling system support (see Fig. 2); F = fan cooling for thermoelectric devices; G = fiber optics; H = UV source connection for 100-μm fiber optics; I = detector head for fiber optics; J = variable-wavelength UV absorbance detector. Commercial suppliers are listed in the Experimental section.

U.S.A.) that thermostated the capillary. The alumina was 99.5% Al_2O_3 with a thermal conductivity of 36 W m^{-1} K^{-1}.

A fused-silica lens (Oriel Corp., Stamford, CT, U.S.A.) was positioned to focus the UV source radiation onto a 600-μm fused-silica fiber optic (Polymicro Technologies, Phoenix, AZ, U.S.A.), which was termed the source fiber optic. Another 600-μm detection fiber optic was press-fitted into the upper side of the alumina holder in order to direct the signal to the photodiode of the detector and is termed the detection fiber optic. The reference fiber optic was a 200-μm fiber that was used without the need of a lens and was connected directly to the reference photodiode. All the fibers were polished (Ealing Electro-optics, Holliston, MA, U.S.A.) and press-fitted into a PTFE tube which was then press-fitted into the cooling system block. At 220 nm, the light loss on a polished fiber optic was about 1 decibel/m, which corresponded to about 80% transmittance[18]. The fiber optics illuminated a detection aperture or slit of 50 μm wide by 200 μm long, or about 900 pl for a 75 μm I.D. capillary.

Samples and running buffers were contained in 0.5-ml polypropylene Eppendorf micro test tubes (Brinkman Instruments, Westbury, NY, U.S.A.). The micro test tubes were mounted on 1/8-in. nylon rods that swung into position around the capillary ends leaving about 0.5 cm of exposed column at each buffer. Platinum wires were positioned on the nylon rod so that when the micro test tube was in place, the electrode was automatically in the buffer solution.

Electronic temperature control was performed with an LDT-5910 thermoelectric temperature controller (ILX Lightwave Corp., Bozeman, MT, U.S.A.) which contained a 10-kΩ thermistor for temperature feedback. Thermal contact of the thermistor and thermoelectric devices to the alumina block was aided with the use of a high temperature thermally conductive paste (Omega Engineering, Stamford, CT, U.S.A.). The paste had a thermal conductivity of 0.7 W m^{-1} K^{-1}. Ethylene glycol, with a thermal conductivity of 0.26 W m^{-1} K^{-1}, was used to enhance the thermal contact of the column to the alumina support. The thermistor calibration was checked for accuracy with a type K thermocouple. Two thermoelectric modules (Cambion, Tampa, FL, U.S.A.) were held on the alumina block by the heat sink which was cooled or warmed with either tap water or forced air convection, depending on the set temperature of the cooling system relative to ambient.

Natural air convection was accomplished with the column suspended between

two buffer reservoirs containing the running buffer. For forced air convection, a 3-in. fan was located 30 cm perpendicular to the column. The air velocity was measured to be 1.5 m/s with a thermo-anemometer (Alnor, Niles, IL, U.S.A.).

The running buffer used for most of the experiments was 100 m*M* Tris, 250 m*M* boric acid and 7 *M* urea at pH 7.6. Also, a 100 m*M* Tris, 25 m*M* boric acid, pH 8.6 buffer was utilized. The buffers were carefully filtered and degassed prior to use. When the sample was dissolved in water, the use of urea and Tris resulted in the detection of a water peak, which was confirmed during the injection of a blank sample. This water peak was used to calculate the electroosmotic velocity in these experiments. This technique was also verified by spiking 1 μl of mesityl oxide in about 1 ml of water, and the resulting absorbance during a run coincided with the injection front. Horse heart myoglobin (Sigma, St. Louis, MO, U.S.A.) was used as supplied and diluted with HPLC grade water to 1 mg/ml, then filtered and degassed.

THEORY

It is important to understand the nature of heat generation as it affects column temperature in HPCE so that an effective temperature control system can be designed, constructed and characterized. The magnitude of the column temperature, as well as the temperature gradients, are proportional to the heat generation rate or power density Q (W/cm^3):

$$Q = VI/(\pi r_1^2 L) = EI/(\pi r_1^2) \tag{1}$$

where V is the applied voltage, I is the current in amperes, E is the applied field (V/L), r_1 is the internal bore radius of the capillary in centimeters and L is the overall length in centimeters[12]. Values for the heat generation rate can reach 1500 W/cm^3 or higher[5], although typical operation is around 300 W/cm^3 (ref. 6).

As a consequence of heat generation, the temperature gradient from the center of the column to the inside of the fused-silica capillary wall can be calculated as[6,12]:

$$\Delta T_c = Qr_1^2/(4\kappa_b) \tag{2}$$

where κ_b is the thermal conductivity of the buffer medium in W cm^{-1} K^{-1}. Since it has been estimated that a temperature gradient of less than 1 K across the column bore should not appreciably affect the efficiency of the separation[12], eqns. 1 and 2 can be combined to obtain a practical relationship between ΔT_c and the power per unit length as

$$EI \leqslant (4\Delta T_c \pi \kappa_b) \leqslant 7.6 \text{ W/m} \tag{3}$$

where ΔT_c = 1 K and κ_b = 0.605 W m^{-1} K^{-1} (thermal conductivity of water). Since at a given field the resulting current is a function of the electrical conductivity of the buffer and the radius of the column, eqn. 3 will hold for any set of column conditions. The important aspect of working with narrow-bore capillaries is that at constant field, the current is lower when the column internal radius is decreased. Consequently, in most applications involving columns of 100 μm I.D. or less, 7.6 W/m is rarely

attained. Furthermore, without a cooling system it has been suggested that operation below 1 W/m results in optimum separation efficiency[19], and therefore ΔT_c is not generally a concern in HPCE, as has been noted previously[4,6,12].

While it can be assumed that a small ΔT_c within the capillary bore will have only a slight effect on efficiency, the actual temperature at the inside wall of the column, T_w, and thus the temperature of the buffer must be considered

$$T_w = T_A + \Delta T_e \tag{4}$$

where ΔT_e is the temperature difference between the inside wall of the capillary and the environment surrounding the capillary, and T_A is the ambient temperature. ΔT_e is given by[12]

$$\Delta T_e = Qr_1^2 [(1/2\kappa_1)\ln(r_2/r_1) + (1/2\kappa_2)\ln(r_3/r_2) + (1/2r_3)(1/h)] \tag{5}$$

where κ_1 and κ_2 are the thermal conductivities of the media (*e.g.* fused silica, polyimide) through which the heat is transferred, and r_1, r_2, r_3 are the capillary inside radius, the outer radius of the fused silica, and the outer radius of the polyimide, respectively. Since ΔT_e is proportional to Qr^2, which has units of W/m, these units will be used as an indication of the heat generation rate in the remainder of the paper.

The thermal transfer coefficient h is indicative of the heat dissipation rate from the outside surface of the capillary to the environment and is in units of $W\ m^{-2}\ K^{-1}$. For the solid-state cooling system the term containing h can be substituted for the materials contained in the cooling system and approximated by

$$(1/2r_3)(1/h) \approx (1/2\kappa_3)\ln(r_4/r_3) + (1/2\kappa_4)\ln(r_5/r_4) \tag{6}$$

where κ_3 and κ_4 are the thermal conductivities of the ethylene glycol and the alumina, and r_4 and r_5 are the outer radii of the ethylene glycol and alumina, respectively. Table I contains the appropriate thermal conductivities and the individual ΔT_e coefficients for the components involved in the present cooling system.

The third column in Table I shows the individual ΔT_e coefficients and the sum of the ΔT_e coefficients for inside diameters of 50, 100 and 200 μm. The ΔT_e coefficients times the power density term (W/m) approximates the temperature drop across the material in question, *i.e.* eqn. 5. Since the outside diameters of the fused silica and polyimide are nearly constant for the Polymicro Technologies tubing, the coefficients for the temperature drop across the polyimide, ethylene glycol and the cooling system did not vary with column internal diameter. Consequently, the sum of the temperature coefficients decrease from 2.6 to 1.7 with increasing internal diameter because of the reduced fused-silica wall thickness. However, this decrease is more than offset by the factor of 8 increase in the quantity of heat generated (at constant E) as a result of the increased diameter of the tubing. When the outer diameter of the capillary is held constant and the internal diameter is increased, the heat is more easily transferred through the capillary wall (which is becoming thinner) but a much greater amount of heat is being generated. Hence, a greater ΔT_e exists due to the increasing generated heat.

In contrast, it can be seen from eqn. 5 that if the internal radius r_1, the poly-

TABLE I

THERMAL CONDUCTIVITIES AND ΔT_e COEFFICIENTS FOR TEMPERATURE CONTROL SYSTEM MATERIALS

NA = Not applicable. The temperature coefficient times the power level in W/m equals the temperature drop across the particular material (see eqn. 5).

Medium	*Variable*	$W\ m^{-1}\ K^{-1}$	$0.5\ (1/\kappa)ln(r_{ii}/r_i)$
Water	κ_b	0.61	NA
Fused-silica	κ_1	1.5	0.65[a], 0.40[b], 0.18[c]
Polyimide	κ_2	0.16	0.27
Ethylene glycol	κ_3	0.26	0.13[d]
Alumina	κ_4	36	0.048[e]
Total			1.1[a], 0.85[b], 0.63[c]

[a] Coefficient for column diameter of 50 μm I.D. × 375 μm O.D.
[b] Coefficient for column diameter of 100 μm I.D. × 375 μm O.D.
[c] Coefficient for column diameter of 200 μm I.D. × 375 μm O.D.
[d] Calculated outside radius for the ethylene glycol of 200 μm from eqn. 6.
[e] Calculated using 6.35-mm radius for the alumina.

imide coating thickness ($r_3 - r_2$), and the thermal transfer coefficient h are held constant, increasing the fused-silica wall thickness results in a lower temperature drop from the inside column wall to the environment (*i.e.* ΔT_e). In short, it is better to use a 50-μm column with a 375-μm outside diameter than one with a 150-μm outside diameter, all else being equal. This improvement is due to a reduction in the insulating influence of the polyimide and an enhancement in thermal transfer to the environment by the increased external surface area. This effect can influence ΔT_e by several degrees if h is small and the power density is large. Therefore, it can be concluded that fused-silica capillaries of narrow inside diameter should be coupled with a large outside diameter for minimal heat generation and improved heat dissipation to the environment.

RESULTS AND DISCUSSION

Cooling system design

The thermoelectric cooling system was designed to incorporate certain features that would be advantageous in a variety of separation conditions. One of these features was the use of fiber optics to decouple the cooling system from the detector[18,20–22] The importance of decoupling is to eliminate any thermal contact of the device with the flow cell support. Operation below ambient temperature with configurations that were not decoupled resulted in baseline fluctuations. In addition, the decoupling offered flexibility in handling, as well as the potential to couple the device readily to an autosampler or fraction collector.

For micropreparative applications, it is desirable that the column support have a minimum distance from the detection region to the collection point, and this region should have similar temperature characteristics to the separation region prior to the detection cell. These two factors reduce any error in predicting the elution of the species of interest from the column. With this in mind, the fiber optic detection region

of the column support was located 1 cm from the end of the column support and about 2 or 3 cm from the column end. When the device was assembled and the buffer reservoirs were in place, less than 1 cm at each end of the column were external to the cooling system or a buffer reservoir. This design minimized the length of uncooled column external to the temperature control system.

The column support material, alumina, was chosen not only for its high thermal conductivity, but also for its lack of electrical conductivity. Electrically conductive support materials in contact with the fused silica are problematical when operating above 10 kV, as grounded conductors must be isolated from the high-voltage reservoir by several inches in order to avoid high-voltage arcing. The alumina column support was contained in a plastic holder, which insulated the support from ambient. The surface area of the holder in contact with the alumina was also reduced in order to decrease the heat capacity of the system so that the set temperature could be attained more rapidly.

The alumina was machined to obtain good thermal contact of the support to the column without sacrificing operating flexibility. The lower plate had two grooves and a well to support columns of variable length in the cooling system, as indicated in Fig. 2. The outside diameter of the fused-silica tubing (Polymicro Technologies) had an adequate tolerance such that internal diameters could be selected with a consistent outside diameter that fit the alumina support grooves. The internal diameters were selectable up to 200 μm with an average outside diameter of 357 μm $\pm$ 1.5% relative standard deviation (n = 8 lots).

The column was coiled in the well, and by varying the number of coils, the column length could be changed in increments of 15 cm. To utilize variable column lengths, a small tolerance in the fit of the column to the top half of the device was required for assembly of the support halves. The grooves in the support held the fused-silica tubing snugly at both ends of the column. When the column was coiled in the well, the tension forced the column against the outside wall of the well resulting in a good thermal contact at that point. To further enhance the thermal contact of the device to the column, thermal paste or ethylene glycol has been tested. The thermal paste, however, contained granules that can score the capillary and increase its fragility, and therefore, ethylene glycol was used in these studies.

The cooling system was contained in a black plexiglass box for three reasons. First, the box insulated the high voltage from the operator and the detector. Second, it

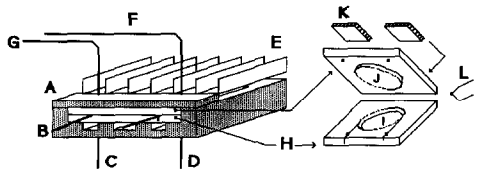

Fig. 2. Expanded view of the thermoelectric cooling system column support: A = black plexiglass holder; B = fused-silica capillary ends; C = 100-μm source fiber optic; D = position of 100-μm reference fiber optic; E = heat sink for thermoelectric devices; F = reference cell 600-μm fiber optic; G = sample cell 600-μm fiber optic; H = alumina plates; I = lower plate with well for column loops; J = upper plate with extension to fit well; K = thermoelectric devices sandwiched between heat sink and alumina plate; L = 10-kΩ thermistor.

limited stray light and third, served as a support for the holder, buffer reservoirs and connections to the electronics.

Cooling system characterization

In order to characterize and compare the efficiencies of heat removal from the column under different cooling conditions, the Ohm's law relationship between applied field and current was studied. For an ideal resistor (where resistance is independent of temperature) the dependence of current on voltage would be linear. However, since the column conductivity will change with temperature, increases in the applied power could cause a deviation in the linear relationship between applied voltage and current. Likewise, if the heat is not efficiently removed from the outer column surface, the temperature buildup within the column bore could result in further deviations from Ohm's law.

The object of a cooling system is to minimize the change in column resistance with the applied electric field by minimizing any change in the outside capillary wall temperature. The cooling system must rapidly remove the generated heat from the outside surface of the capillary. Consequently, with good temperature control the major source of deviation from Ohm's law would be due to the temperature gradient from the column center to the outer surface of the capillary wall coating which, as previously noted, is relatively small under most HPCE operating conditions[6,12]. Since the primary consequence of inefficient cooling at the outer surface of the capillary is the rise of temperature in the entire column, the Ohm's law relationship was used to characterize different methods of cooling by examining the dependence of current on applied field.

In this work, the thermoelectric temperature control system was compared to two other methods of heat removal: natural and forced air convection. Natural convection was studied on a column suspended between two buffer reservoirs with no forced air movement. Suspended in this way, only the air convection caused by the hot column and any small air currents normally present in the laboratory would affect the column resistance. For this experiment the room air conditioning was turned off as it had a significant influence on the linearity of the natural convection plots (*e.g.* Fig. 3 below).

Forced air convection was accomplished with the use of a fan located 30 cm from the same suspended column. The fan was measured to deliver approximately 1.5 m/s of air over the column surface. Although it has been shown that 10 m/s or greater of air velocity would provide improved heat dissipation[6], 1.5 m/s is typical for the fans conveniently available for forced air convection in a general HPCE separation. The columns in these experiments had no detector attached, and therefore, the natural and forced air convection cooling results were more efficient than with an in-line UV detector. If a detector were present, and only the separation portion of the column were cooled, there would not be constant column resistance over the length of the column, and greater deviations from Ohm's law would be expected to occur. In effect, any deviation from Ohm's law could result in inaccurate or irreproducible mobility measurements due to the error in estimation of the viscosity present in the separation portion of the column. Likewise, for accurate collection of a given species in micropreparative applications, as noted above, the length of uncooled column before and after the detector should be minimized.

Current stability

At constant field, the method of cooling can have a significant effect on the stability of the system. Fig. 3 shows the current stability for the three methods of column cooling with a 100-μm column at 500 V/cm with the 100 m*M* Tris, 250 m*M* boric acid, 7 *M* urea buffer. For the three columns, the resulting applied powers were 2.7, 1.9 and 1.3 W/m for natural convection, forced air convection and solid-state cooling, respectively. These applied powers vary because of the different column temperatures resulting from the changes in the thermal transfer rates. The set temperature of the solid-state cooling system was the same as the room air temperature of 23°C. These plots demonstrate the stability of column resistance under constant voltage conditions over the duration of a typical run. The solid state cooled column, trace C, had the least deviation in current of the three methods of cooling. Likewise, trace B (fan cooled) exhibited a lower peak to peak deviation in the current level than trace A. Clearly, the better the control of column temperature, the lower the deviation in current during a run. The principal reason for the stability of the thermoelectric cooling system was that the temperature regulation was under proportional current control, *i.e.* the thermoelectric devices were always on and the applied current to the devices changed in response to the temperature feedback. Less expensive on/off type control units can result in detector baseline fluctuations and conductivity changes. Fig. 3 highlights the need to efficiently remove heat in order to control column conditions.

Another important aspect of Fig. 3 is the change in current when the room air conditioning was started. The change in temperature and air convection in the immediate environment around the capillary was responsible for the deviations in the baseline of trace A. Trace B, on the other hand, is affected less than trace A by the air conditioner. This is because the air convection associated with the air conditioner is much less than that resulting from the fan. Therefore, only the temperature change in the room is responsible for the baseline change in trace B. It should be emphasized that this figure shows the importance of both the effect of efficient heat removal, as well as column temperature regulation for maintaining constant column resistance. In short, the column should be isolated from changes in the laboratory environment.

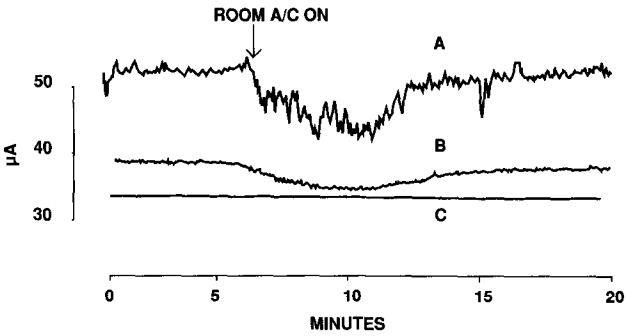

Fig. 3. The stability of current with time. The current is monitored at 500 V/cm for (A) natural air convection, (B) forced air convection, and (C) solid state thermoelectric cooling. Buffer: 0.1 *M* Tris, 0.25 *M* boric acid, 7 *M* urea, pH 7.6. Column: 180 mm × 100 μm. The differences in current levels are the result of the variances in the efficiencies of heat removal (see text). A/C = Air conditioning.

This latter point is most important when operating at constant field. If a cooling system is not available, constant current operation can result in a somewhat self-compensating effect of decreasing voltage with increasing column temperature[8,23]. However, a system operating without temperature control, even under constant current control, may not be adequately defined for accurately assigning mobilities.

The column temperature can be deduced from Fig. 3 and from the Ohm's law plots (Figs. 4–6) for a 100 μm I.D. column under the same buffer conditions. It can be assumed that there are no temperature effects when very low power levels are applied to the system (*e.g.* 0.025 W/m)[8]. From current generated at low power levels, Ohm's law was used to predict the current level at 500 V/cm. The actual current was slightly less than a 2% deviation from the predicted value indicating that the column temperature was less than 1°C higher than the set temperature of the cooling system, or about 24°C. It was also calculated from Fig. 3 that the temperature of the natural convection was 33°C higher than the column temperature in the solid-state cooling system or an actual temperature of about 57°C. Furthermore, the difference in temperature between the forced air cooling and the solid state cooling was about 9°C, or a column temperature of roughly 33°C. These temperature levels compare well with that which was predicted or measured previously[5,6].

The reason for these different column temperatures as a function of the method of cooling (at constant field) are the variations in the ability of the system to remove the heat from the outer surface of the capillary, *i.e.* differences in the thermal transfer coefficients h. The values of h are determined, as described in the Theory section, from the temperature increases ΔT_e in Fig. 3 with eqn. 5. Table II shows the h and ΔT_e values for the three cooling systems at increasing applied powers. Included are typical fields, currents and applied powers. It may be noted again that powers less than 1.0 W/m have been recommended for minimizing Joule heating effects[19].

Interestingly, Table II shows that for fan cooling and natural convection at 1

TABLE II

DEPENDENCE OF ΔT_e ON COOLING SYSTEM METHOD AND APPLIED POWER

h = Thermal transfer coefficient; ΔT_e = temperature difference between the inside wall of the capillary and the environment around the capillary.

Cooling method	h ($W\,m^{-1}\,°C^{-1}$)	*Power (W/m)*	ΔT_e
Natural convection	70	0.5 (30 kV/m)(16 μA)[a]	6.2
		1.0 (30 kV/m)(33 μA)	12.4
		2.5 (30 kV/m)(83 μA)	31.2
		5.0 (30 kV/m)(167 μA)	62.5
Forced air convection	180	0.5	2.5
		1.0	5.0
		2.5	12.5
		5.0	25.0
Solid-state cooling	2600	0.5	0.3
		1.0	0.6
		2.5	1.5
		5.0	3.0

[a] Example of field and current that results in particular power level.

W/m the column temperature can be 5°C or 12°C above ambient, respectively. The differences in electrophoretic mobility from ambient would then be estimated to be 25% and 10%, respectively, assuming 2%/°C variation in mobility[8]. On the other hand, at the same applied power the ΔT_e is only 0.6°C with the Peltier device for a mobility difference of roughly 1%. Thus, even at the limit of 1 W/m, active and efficient cooling is required. In addition, at higher powers of 2.5 and 5 W/m which can be found in a variety of applications, very large increases in column temperature can be realized. In these situations, an effective cooling device is mandatory.

Without the use of an efficient cooling system there is concern that the species of interest may thermally degrade. Column temperatures under some natural and forced air convection conditions may be sufficient to denature some proteins. Similarly, if the analytical accuracy for migration times performed in different laboratories is to be within certain limits, for example ±2%, reproducibility of absolute temperature must be better than ±1°C, since, as noted, mobilities vary by about 2%/°C. In recording laboratory data, it is recommended that a record of the applied field, current level, cooling method and set temperature, be included with the usual experimental conditions.

Ohm's law plots

The three modes of heat removal were further compared by studying the dependence of current on applied voltage (*E–I* plots), and the results are shown in Figs. 4–6. A positive deviation from linearity due to the column temperature increase is observed at high fields. This behavior can be best described in terms of a second or third order polynomial rather than with a linear regression line. These plots show the effect of varying the column diameter on the dependence of current on applied voltage.

Fig. 4 shows the *E–I* plots for 50, 100 and 200 μm column diameters with natural air convection. In each case there was a significant curvature due to the decreasing column resistance with increasing field. In the 200-μm column the current became unstable above 200 μA and 200 V/cm (4 W/m), probably due to excessive

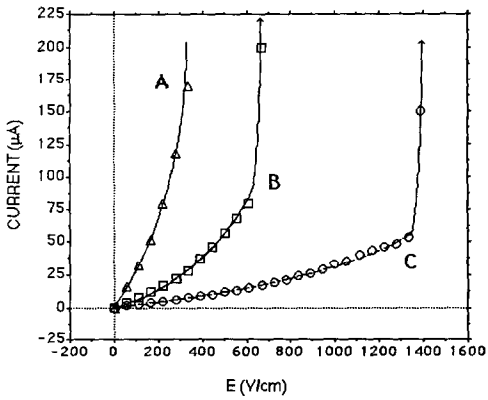

Fig. 4. Ohm's law plot of current *vs.* electric field for natural convection on a 180-mm capillary column length with internal diameters of (A) 200 μm; (B) 100 μm; (C) 50 μm. The buffer was the same as in Fig. 3. The rapid rise in current at high voltage indicates the point of thermal breakdown where the rate of heat generation is greater than heat removal.

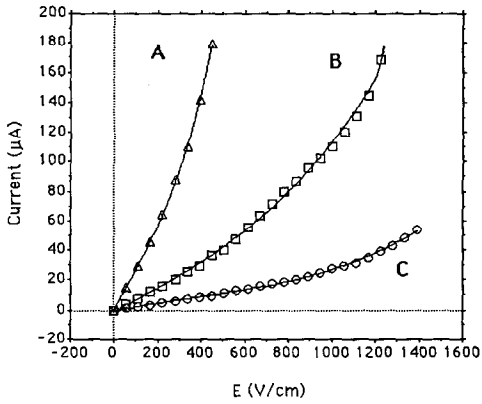

Fig. 5. Ohm's law plot for forced air cooling on a 180-mm capillary column length with internal diameters of (A) 200 μm; (B) 100 μm; (C) 50 μm. The buffer was the same as in Fig. 3.

temperatures which resulted in air or vapor bubble formation in the column. The highest voltage point for the 50-μm and the 100-μm columns in Fig. 4 was also not a stable current reading, but simply the last current recorded before the power supply was shut off. At this point, the column was no longer capable of removing the heat generated by the applied power, and thermal breakdown occurred. The solution increased in temperature as the resistance fell (*i.e.* temperature feedback) until the circuit was broken. Under these conditions, a 50-μm column was able to handle fields up to 1300 V/cm or about 7 W/m. Although this figure shows that narrow-bore columns are more linear than the wider bore columns, the 50-μm column still shows curvature, as seen in Fig. 7.

Fig. 5 presents the results of a similar experiment with a forced air fan cooled column. The useful range of applied field was increased relative to Fig. 4 as no thermal breakdown was observed. Also, the linearity (or constancy of column resistance) was improved for each of the column diameters. The 200-μm column was still unstable above about 200 μA, but this current level was not reached until 440 V/cm

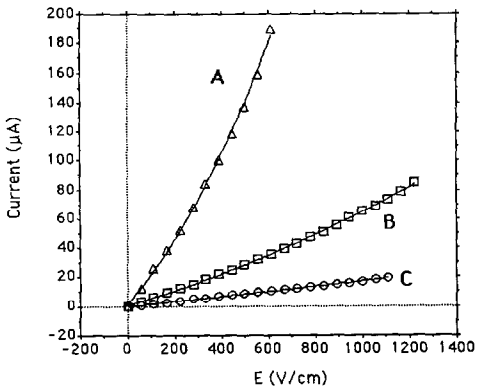

Fig. 6. Ohm's law plot for Peltier thermoelectric cooling at 20°C, 180-mm capillary column length and internal diameters of (A) 200 μm; (B) 100 μm; (C) 50 μm. The buffer was the same as in Fig. 3.

(110 V/cm higher than with natural air convection). For operation with these column diameters, fan cooling was a definite improvement over natural convection.

Ohm's law plots for the thermoelectrically cooled columns of different diameters which were thermostated at 20°C are shown in Fig. 6. In the case of the 200-μm column, the applied field at 200 μA was over 600 V/cm. Also, the linearity of each of the plots was enhanced by using the solid-state temperature control system as compared to natural or forced air convection. Furthermore, there was no indication of thermal breakdown as in Fig. 4.

In order to compare the three cooling methods according to their abilities to remove heat, a plot of the residuals of current *vs.* field for the 50-μm capillary was constructed as shown in Fig. 7. A residual is the deviation of a data point from the linear least squares best fit line of the data. The three data sets were fitted to a line over the same range of applied fields so that a valid comparison could be made. Under these conditions, a residuals plot is a good indication of whether the deviation of the data from the best fit line is random or non-random. This method has been used previously to indicate non-linear behavior of calibration plots in HPLC[24].

Fig. 7 shows that even for the 50-μm column there was significant non-random deviation from the line when the column was cooled by natural or forced air convection. On the other hand, the non-linearity was only a few tenths of a microampere for the thermoelectrically cooled system. From these results, the major deviation from Ohm's law was inefficient heat removal from the outside wall of the capillary to the environment, as noted earlier[6]. The residual plots for the 100-μm and 200-μm columns were similar but the residuals were greater, indicating that the temperature effects were even more severe.

Variable column temperature

The ability to vary column temperature is as important as the ability to maintain constant temperature. The importance of column temperature variation, for example, is seen in being able to manipulate chemical equilibria such as metal chela-

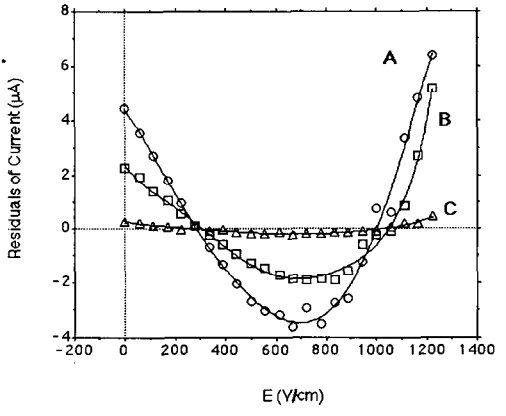

Fig. 7. Plot of the residuals of current *vs.* field for 50-μm columns under (A) natural air convection, (B) forced air convection and (C) thermoelectric cooling from experiments shown in Figs. 4–6. A residual is the deviation of an individual *E–I* data point from the linear best fit line of all the data. The plots provide a comparison of the Ohm's law deviations for the three cooling methods employed.

tion and micelle partitioning[4,13]. Moreover, separations below ambient temperature have been shown to be useful in avoiding proteolysis or sample decomposition[25]. On the other hand, oligonucleotide separations have been altered by injecting at 60°C, where the species adopt a random coil configuration[26].

Fig. 8 shows the relationship of varying column temperature on the *E–I* plots for a 50-μm capillary. The plots support the expected relationship of about 2% increase in conductivity per degree centigrade (*e.g.* the field that produced 10 μA at 30°C produced 12 μA at 40°C for a 20% increase with a 10°C change). At 10°C, the field could only be extended to 700 V/cm or about 12 kV because of condensation on the alumina block. Since the detector was decoupled from the cooling system, it should be possible to reduce the humidity of the environment in the housing and extend the usable temperature to lower values. It should also be noted that the operation of the thermoelectric device at lower temperatures resulted in lower power dissipation for a given field and buffer concentration, and therefore, a lower ΔT_e.

Of additional significance in Fig. 8 was that the current level for the 50-μm column at 30°C and 330 V/cm was the same as that experienced for a given field in the forced air convection experiment from Fig. 5, run at ambient temperature of 23°C. Likewise, the current level at 33 V/cm and 40°C was roughly that of the current level at the same field with natural air convection of Fig. 4. This result further supports the conclusion that, in general, a 50 μm I.D. column will not sufficiently minimize Joule heating without the incorporation of an efficient cooling system.

A further consequence of changing column temperature with increasing field is that the electroosmotic flow will not be linearly dependent on the field[27,28]. This non-linearity is due to the dependence of the electroosmotic flow on the viscosity in the double layer near the wall[8]. Fig. 9 shows the relationship of electroosmotic velocity *vs.* field up to 800 V/cm for the solid state cooling system at 20°C. The velocity of a water injected peak was measured in the same Tris–boric acid–urea buffer as in Fig. 3.

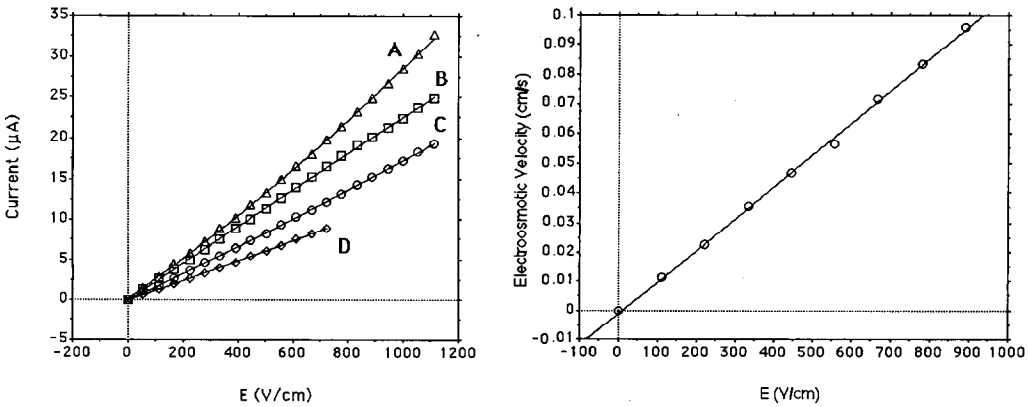

Fig. 8. Ohm's law plots for Peltier thermoelectric temperature control on a 180 mm × 50 μm capillary column. (A) 40°C; (B) 30°C; (C) 20°C; (D) 10°C. The buffer was the same as in Fig. 3.

Fig. 9. Plot of electroosmotic velocity *vs.* applied field at 20°C. The buffer was the same as in Fig. 3. The plot is linear (*i.e.* did not show large non-random deviations) with a correlation coefficient of greater than 0.995, indicating control of the double layer temperature.

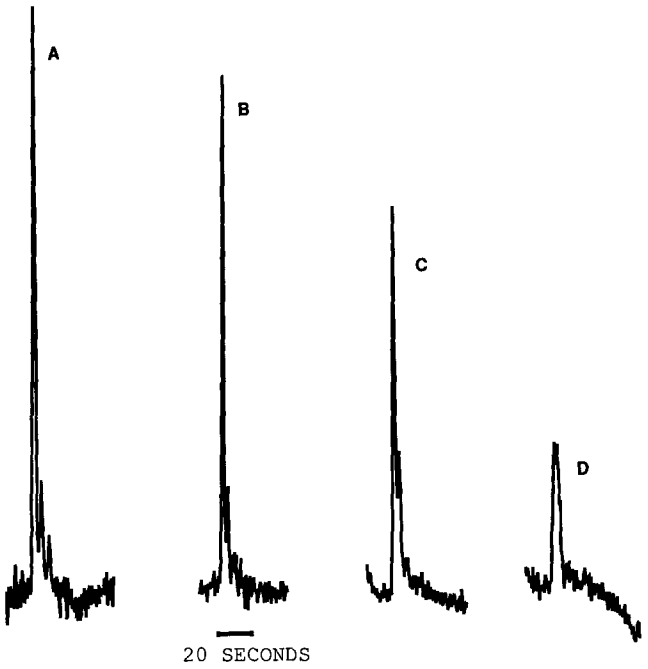

Fig. 10. The dependence of horse heart myoglobin peak shape on column temperature. Column conditions were total length 340 mm, effective length 320 mm, 75 μm I.D. capillary column. Operation was under constant current at 9.5 μA with applied fields of 500, 430, 390 and 320 V/cm at 20, 30, 40 and 50°C, respectively. The buffer was 0.1 *M* Tris and 0.025 *M* boric acid pH 8.6, with detection at 220 nm.

The plot, passing through zero, was quite linear with a correlation coefficient of greater than 0.995, indicating that the temperature of the inside wall of the capillary was nearly constant over the range of applied voltage. Although operating under constant control compensates for temperature changes in the double layer[5,8], it is preferable to operate under constant voltage with temperature control so that electrophoretic mobilities can be accurately assigned.

As already noted, another consequence of inefficient column temperature regulation is that the overall temperature of the column, as a result of Joule heating, could cause enhanced peak broadening. As an example of this behavior, Fig. 10 shows a sample of horse heart myoglobin which was injected at different column temperatures (controlled by the solid state cooling system). The separation was run at constant current of 9.5 μA in order to minimize the effect of changing temperature on the migration time[8]. In this experiment the applied power was 0.5 W/m at 20°C and decreased to 0.3 W/m at 50°C. The observed decrease in peak height and the increase in peak width in Fig. 10 with increasing temperature may be due to sample denaturation at the higher temperatures. It should also be noted that the potential temperatures with high conductivity buffers on an inefficiently cooled column could easily reach the elevated temperatures demonstrated in this experiment, inadvertently causing a similar loss in efficiency (see Table II).

CONCLUSIONS

The incorporation of a temperature control system with a high thermal transfer coefficient is important for maintaining constant column resistance, optimizing separation efficiency, reducing sample decomposition, or maintaining a desired chemical equilibria. Efficient removal of heat at high fields can minimize a number of detrimental effects on column performance such as current instability, convection, deformation of electrophoretic zone profile, or diffusion.

It is important to consider temperature control not only in terms of efficient heat removal, but also as a column thermostat for manipulation of column temperature. Although the use of smaller column diameters will reduce the effects of Joule heating on separations, the control of temperature is still important in maintaining chemical equilibria and, therefore, reproducibility of interlaboratory results. In addition, the ability to vary the column temperature permits the manipulation of separation selectivity through the control of chemical equilibria. Furthermore, since electrophoretic mobilities change 2%/°C, acceptable reproducibility between laboratories could be difficult without accurate control of the desired column temperature during the separation. For this reason, it is important that the record of separation conditions contain the method of cooling, the field, and the current that resulted in a given separation in order to provide an indication of the level of thermal effects that might be present.

ACKNOWLEDGEMENTS

The authors gratefully acknowledge support by Beckman Instruments, Inc., and the James L. Waters Chair in Analytical Chemistry. The authors further thank Dr. Carlos Diez-Masa for initial studies in this area. This paper is contribution No. 387 from the Barnett Institute of Chemical Analysis and Materials Science.

REFERENCES

1 J. W. Jorgenson and K. DeArman Lukacs, *Science (Washington, D.C.)*, 222 (1983) 266.
2 M. J. Gordon, X. H. Huang, S. L. Pentoney, Jr. and R. N. Zare, *Science (Washington, D.C.)*, 242 (1988) 224.
3 B. L. Karger, A. S. Cohen and A. Guttman, *J. Chromatogr.*, 492 (1989) 585.
4 S. Terabe, K. Otsuka and T. Ando, *Anal. Chem.*, 61 (1989) 251.
5 S. Terabe, K. Otsuka and T. Ando, *Anal. Chem.*, 57 (1985) 834.
6 J. H. Knox, *Chromatographia*, 26 (1988) 329.
7 J. H. Knox and I. H. Grant, *Chromatographia*, 24 (1987) 135.
8 S. Hjertén, *Chromatogr. Rev.*, 9 (1967) 122.
9 J. O. N. Hinkley, *J. Chromatogr.*, 109 (1975) 209.
10 J. F. Brown and J. O. N. Hinkley, *J. Chromatogr.*, 109 (1975) 218.
11 F. Foret, M. Deml and P. Boček, *J. Chromatogr.*, 452 (1988) 601.
12 E. Grushka, R. M. McCormick and J. J. Kirkland, *Anal. Chem.*, 61 (1989) 241.
13 A. S. Cohen, S. Terabe, J. A. Smith and B. L. Karger, *Anal. Chem.*, 59 (1987) 1021.
14 R. M. McCormick, *Anal. Chem.*, 60 (1988) 2322.
15 J. Jorgenson, presented at the *1st International Symposium on High Performance Capillary Electrophoresis, Boston, MA, April 10–12, 1989.*
16 R. C. Allen and C. A. Saravis, *Biotechniques*, 5 (1987) 248.
17 *Model EC1001*, E-C Apparatus Corporation, St. Petersburg, FL, 1988.

18 *Optical Fiber Data Sheet*, Polymicro Technologies, Phoenix, AZ, 1987.
19 M. J. Sepaniak and R. O. Cole, *Anal. Chem.*, 59 (1987) 472.
20 A. E. Bruno, E. Gassmann, N. Pericles and K. Anton, *Anal. Chem.*, 61 (1989) 876.
21 F. Foret, M. Deml, V. Kahle and P. Boček, *Electrophoresis*, 7 (1986) 430.
22 E. Gassman, J. E. Kuo and R. N. Zare, *Science (Washington, D.C.)*, 230 (1985) 813.
23 G. O. Roberts, P. H. Rhodes and R. S. Snyder, *J. Chromatogr.*, 480 (1989) 35.
24 M. F. Delaney, *LC, Mag. Liq. Chromatogr. HPLC*, 3 (1985) 264.
25 C. A. Saravis, R. C. Allen, P. Thomas and N. Zamcheck, in V. Neuhoff (Editor), *Electrophoresis 1984*. Verlag Chemie, Weinheim, 1984.
26 A. S. Cohen, D. Najarian, J. A. Smith and B. L. Karger, *J. Chromatogr.*, 458 (1988) 323.
27 C. F. Simpson and K. D. Altria, *Anal. Proc.*, 23 (1986) 453.
28 K. D. Altria and C. F. Simpson, *Chromatographia*, 24 (1987) 527.